BIOCHEMISTRY

 Volume 47, Number 35 September 02, 2008

Rapid Reports

Crystal Structure of Type 2 Isopentenyl Diphosphate Isomerase from *Thermus thermophilus* in Complex with Inorganic Pyrophosphate[†]

Jérôme de Ruyck,*[,‡] Jenny Pouyez,[‡] Steven C. Rothman,[§] Dale Poulter,[§] and Johan Wouters*[,‡]

Department of Chemistry, University of Namur, Namur, Belgium, and Department of Chemistry, University of Utah, Salt Lake City, Utah 84112

Received June 20, 2008; Revised Manuscript Received August 4, 2008

ABSTRACT: The N-terminal region is stabilized in the crystal structure of *Thermus thermophilus* type 2 isopentenyl diphosphate isomerase in complex with inorganic pyrophosphate, providing new insights about the active site and the catalytic mechanism of the enzyme. The PP_i moiety is located near the conserved residues, H10, R97, H152, Q157, E158, and W219, and the flavin cofactor. The putative active site of isopentenyl diphosphate isomerase 2 provides interactions for stabilizing a carbocationic intermediate similar to those that stabilize the intermediate in the well-established protonation−deprotonation mechanism of isopentenyl diphosphate isomerase 1.

Isopentenyl diphosphate isomerase (IDI) is a key enzyme in the isoprenoid biosynthetic pathway, which produces several classes of essential compounds in humans. IDI catalyzes the required isomerization of isopentenyl diphosphate (IPP) to dimethylallyl diphosphate (DMAPP) in the entry of mevalonate into the isoprenoid pathway and serves to balance the pools of IPP and DMAPP in the methylerythritol phosphate entry (*1, 2*).

Two isoforms of IPP isomerase, IDI-1 and IDI-2, have been identified. IDI-1 is a zinc metalloprotein which was first characterized more than 40 years ago (*3*−*5*). The structure of IDI-1 is known, and its mechanism of action has been studied extensively (*6*−*8*). The IDI-2 isoform was discovered recently (*9*). The enzyme is a flavoprotein that requires FMN, a reducing agent (typically NADPH), and a divalent metal. IDI-2 is an essential enzyme for those pathogenic microorganisms, such as some strains of *Streptococcus* and *Staphylococcus*, that rely on the mevalonate pathway for isoprenoid biosynthesis (*10*). Thus, IDI-2 is a logical target for the design of anti-infectious agents.

There are various proposals for the role of the flavin, although recent reports suggest that the cofactor participates in a protonation−deprotonation mechanism (*11*−*14*). A crystal structure of the *Bacillus subtilis* protein (*bs*-IDI2) was reported in 2003 (PDB entry 1P0N) (*15*). In 2004, two structures of IDI-2 from *Thermus thermophilus* (*tt*-IDI2), a thermophilic microorganism, were determined (PDB entries 1VCF and 1VCG) (*16*). The proteins crystallized as typical $\alpha 8/\beta 8$ TIM barrels, and one molecule of FMN was bound per monomer. Nevertheless, electron density was not detected for several amino acids at the active site due to their conformational flexibility. We obtained an X-ray structure of *tt*-IDI2 in 2005 and faced the same problem with flexibility. We therefore combined the available structural information to construct a model of the complete structure of IDI-2 (PDB entry 2IOW). Docking studies with this model helped us to identify a putative active site (*17*). In this report, we present an experimental X-ray structure of IDI-2 from

[†] J.d.R. is grateful for financial support from the Belgian Fonds pour la formation à la Recherche dans l'Industrie et dans l'Agriculture (FRIA). Financial support from NIH Grant GM 25521 (CDP) and FNRS (IISN 4.4505.00) for access to the ESRF synchrotron is acknowledged.

* To whom correspondence should be addressed. Telephone: +32 81 72 4569. Fax: +32 81 72 4530. E-mail: jerome.deruyck@fundp.ac.be or johan.wouters@fundp.ac.be.

[‡] University of Namur.

[§] University of Utah.

10.1021/bi801159x CCC: $40.75
Published on Web 08/12/2008

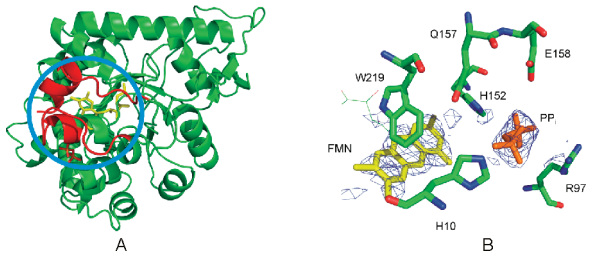

FIGURE 1: (A) Typical α8β8 TIM barrel fold of one monomer. Red segments are flexible regions (9−22 and 223−234) observed in this structure and absent in 1P0N and 1VCG. Flavin (yellow, A and B) is located at the end of the barrel and near PP_i (orange, B). (B) Extra electron density (blue contour, $2F_o - F_c$, 1σ) corresponding to PP_i is observed near the flavin and conserved histidines His 10 and His 152. The indole group of W219 interacts with the isoalloxazine moiety through an edge-to-face interaction, and the N-terminal segment, which contains His 10, is well-folded. All figures were prepared using PyMOL (*21*).

Table 1: Data Collection and Refinement Statistics

space group	$P3_2$	completeness[a] (%)	97.3 (84.0)
cell dimensions (Å)	$a = 142.5$, $b = 142.5$, $c = 109.7$	R_{merge}[a] (%)	12.4 (32.0)
wavelength (Å)	0.9797	I/σ[a] (I)	7.1 (3.4)
highest resolution (Å)	2.97	R_{work}/R_{free}[b] (%)	21.1/29.2
no. of observed reflections	291921	rmsd	
no. of unique reflections	49971	bond lengths (Å)	0.02
PDB entry	3DH7	bond angles (deg)	2.02

[a] Values listed in parentheses are for the highest-resolution shell (3.15−2.97 Å). [b] The free test subset represents 5% of the total number of unique reflections.

T. thermophilus in complex with inorganic pyrophosphate (PP_i) (PDB entry 3DH7), which facilitates visualization of electron density for a conserved region at the N-terminus of the protein. Analysis of the electron density maps and molecular modeling with this more complete structure present new perspectives for the mechanisms of catalysis and inhibition of IDI-2.

Overexpression, purification, and crystallization of *tt*-IDI2 were adapted from the previous experimental procedures (*17*) and are described in the Supporting Information. The protein also crystallizes as a typical α8β8 TIM barrel (Figure 1A). Four monomers are assembled as a symmetrical *D*4 open cage-like structure in the asymmetric unit, similar to 1VCG. Main crystallographic details are given in Table 1.

As previously described (*14*), one molecule of FMN is bound per monomer and located in the standard phosphate binding (SPB) region of the TIM barrel. The phosphate moiety of the cofactor is stabilized by interactions with Gly 264, Tyr 266, and Ala 285, while the isoalloxazine ring contacts Leu 11, Ala 65, Met 66, Ser 95, Asn 123, Lys 187, and Val 189. The *si* face of FMN faces the indole moiety of Trp 219 and is further stabilized via an edge-to-face interaction.

After refinement of the position of the cofactor, we observed an additional electron density located near the flavin that was attributed to inorganic pyrophosphate (PP_i). The structure of the IDI-2·flavin·PP_i complex (Figure 1B) allows us to identify conserved residues in the putative active site. PP_i is stabilized by electrostatic interactions with conserved residues His 10, Arg 97, and His 152 and is located near Gln 157, Glu 158, and FMN. It is noteworthy that comparisons of the available crystal structures for IDI-2 reveal two different conformations for the aromatic Trp 219 residue.

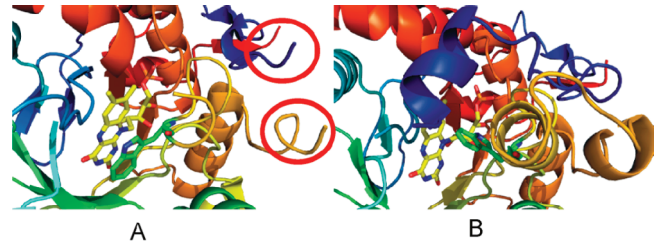

FIGURE 2: (A) In the IDI-2·FMN complex, Trp 219 (green) stacks with the isoalloxazine ring (yellow). Some parts of the enzyme are very flexible and cannot be observed by X-ray diffraction (red circles). We assume that this is the opened state of IDI-2. (B) In the IDI-2·FMN·PP_i complex, Trp 219 interacts with FMN through an edge-to-face interaction, the global fold of the enzyme is stabilized, and the previously missing parts are observed. This corresponds to a closed state triggered by the substrate binding.

In the apoprotein, the indole ring of tryptophan stacks with the isoalloxazine ring (1VCF) (Figure 2A), the N-terminal segment is disordered, and residues 1−22 are not seen. When PP_i is bound, Trp 219 interacts with FMN via an edge-to-face interaction, and additional N-terminal residues 9−22 are visible in the electron density map (Figure 2B). We conclude that the enzyme exists in an "open" form in the absence of substrate. Substrate binding triggers a conformational change to a "closed" form where the N-terminal residues form a lid over the putative active site that shield it from bulk water.

Recent reports about irreversible inhibitors of IDI-2 demonstrated that the compounds covalently modified the isoalloxazine ring of reduced FMN (*18*−*20*). On the basis of our new crystallographic structure, we modeled the binding of oIPP to the IDI-2·FMN complex; oIPP is a potent active site-directed irreversible inhibitor. We observed (Figure 3A) that the epoxide ring of oIPP is located just above N5 of FMN (N5−C_{asym} distance, 4.1 Å). This binding mode is fully compatible with an irreversible inhibition where N5 acts as the nucleophile after the epoxide ring is activated by protonation. Support for this model was achieved by treating crystals of the IDI-2·FMN complex with 100 mM $Na_2S_2O_4$ followed by 10 mM oIPP. Upon addition of $Na_2S_2O_4$, we observed that the yellow color vanished, indicating that FMN was reduced. Due to the ambient O_2, the flavin slowly reoxidized and the yellow color of the crystals reappeared. However, when the reduced crystals were soaked with oIPP, they remained colorless, suggesting that flavin is locked in its reduced form and that oIPP chemically modified the isoalloxazine ring (Figure 3B).

This observation is in agreement with UV−vis spectral observations in solution for epoxide-mediated inactivation of IDI-2 (*12, 14*).

Those new results are consistent with the hypothesis that IDI-1 and -2 catalyze isomerization by similar protonation−deprotonation mechanisms (Figure 3C) (*12, 18*−*20*). The putative carbocationic intermediate, generated after the protonation step, could be stabilized by π−cation interactions with the isoalloxazine ring in FMN and the indole ring in W219. Similar interactions between the carbocation and a conserved tryptophan are thought to be important in the protonation−deprotonation reaction catalyzed by IDI-1 (*7*).

To validate the binding mode of oIPP in the active site of IDI-2, we have planned experimental X-ray data collections. A crystal structure of the IDI-2·FMN·oIPP complex would

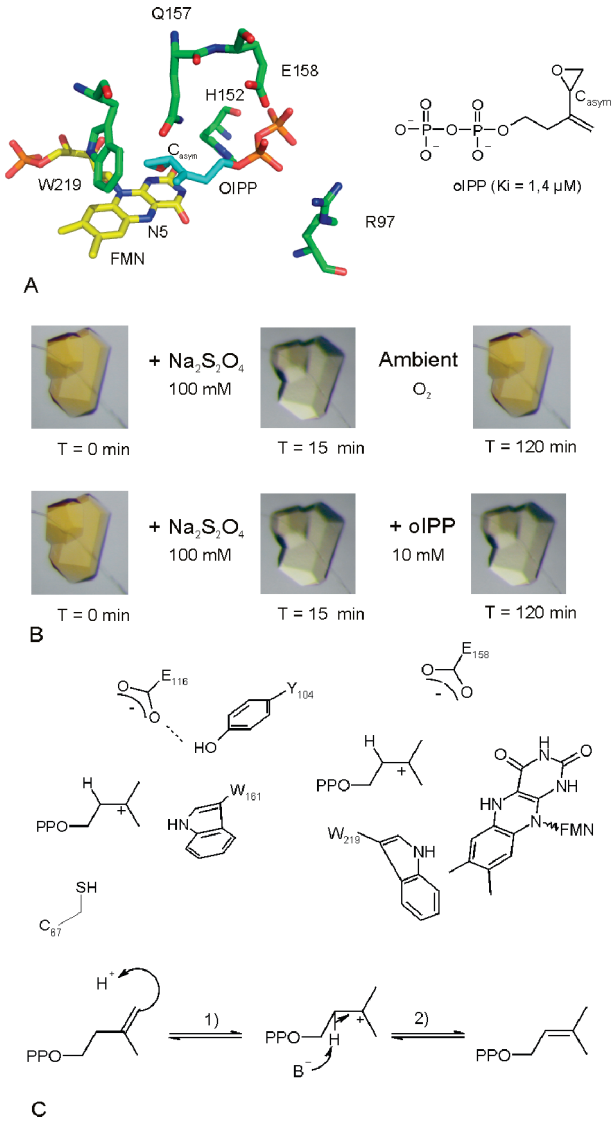

FIGURE 3: (A) Mode of binding of oIPP (light blue) in the putative active site of IDI-2. The epoxide ring is located to chemically modify N5 of the isoalloxazine ring (yellow). (B) Chemical reduction of IDI-2 crystals followed by soaking of oIPP indicates that the flavin cofactor is locked in its reduced form. This is in good agreement with a covalent bond between N5 of flavin and the irreversible inhibitor. (C) Protonation−deprotonation mechanism for isomerization catalyzed by IDI-1 and -2. Aromatic $\pi-\pi$ interactions in IDI-1 and -2 can stabilize the carbocationic intermediate. Reduced FMN could act as the proton donor and/or proton acceptor in the reaction.

provide a strong argument in favor of the hypotheses about the catalytic and inhibition mechanisms presented here.

ACKNOWLEDGMENT

We thank all the FIP-BM30A staff for their assistance during data collection.

SUPPORTING INFORMATION AVAILABLE

Overexpression, purification, crystallization, X-ray crystallographic data collection, structure refinement, and molecular modeling. This material is available free of charge via the Internet at http://pubs.acs.org.

REFERENCES

1. Rohmer, M. (1999) *Nat. Prod. Rep. 16*, 565–574.
2. Rohdich, F., Bacher, A., and Eisenreich, W. (2004) *Bioorg. Chem. 32*, 292–308.
3. Agranoff, B. W., Eggerer, H., Henning, U., and Lynen, F. (1960) *J. Biol. Chem. 235*, 326–332.
4. Ramos-Valdivia, A. C., van der Heijden, R., Verpoorte, R., and Camara, B. (1997) *Eur. J. Biochem. 249*, 161–170.
5. Carrigan, C. N., and Poulter, C. D. (2003) *J. Am. Chem. Soc. 125*, 9008–9009.
6. Wouters, J., Oudjama, Y., Ghosh, S., Stalon, V., Droogmans, L., and Oldfield, E. (2003) *J. Am. Chem. Soc. 125*, 3198–3199.
7. Wouters, J., Oudjama, Y., Barkley, S. J., Tricot, C., Stalon, V., Droogmans, L., and Poulter, C. D. (2003) *J. Biol. Chem. 278*, 11903–11908.
8. Durbecq, V., Sainz, G., Oudjama, Y., Clantin, B., Bompard-Gilles, C., Tricot, C., Caillet, J., Stalon, V., Droogmans, L., and Villeret, V. (2001) *EMBO J. 20*, 1530–1537.
9. Kaneda, K., Kuzuyama, T., Takagi, M., Hayakawa, Y., and Seto, H. (2001) *Proc. Natl. Acad. Sci. U.S.A. 98*, 932–937.
10. Kuzuyama, T., and Seto, H. (2003) *Nat. Prod. Rep. 20*, 171–183.
11. Rothman, S. C., Helm, T. R., and Poulter, C. D. (2007) *Biochemistry 46*, 5437–5445.
12. Hoshino, T., Tamegai, H., Kakinuma, K., and Eguchi, T. (2006) *Bioorg. Med. Chem. 14*, 6555–6559.
13. Hemmi, H., Ikeda, Y., Yamashita, S., Nakayama, T., and Nishino, T. (2004) *Biochem. Biophys. Res. Commun. 322*, 905–910.
14. Rothman, S. C., Johnston, J. B., Lee, S., Walker, J. R., and Poulter, C. D. (2008) *J. Am. Chem. Soc. 130*, 4906–4913.
15. Steinbacher, S., Kaiser, J., Gerhardt, S., Eisenreich, W., Huber, R., Bacher, A., and Rohdich, F. (2003) *J. Mol. Biol. 329*, 973–982.
16. Wada, T., Park, S.-Y., Tame, R. H., Kuramitsu, S., and Yokoyama, S., unpublished results, 2003.
17. de Ruyck, J., Rothman, S. C., Poulter, C. D., and Wouters, J. (2005) *Biochem. Biophys. Res. Commun. 338*, 1515–1518.
18. Johnston, J. B., Walker, J. R., Rothman, S. C., and Poulter, C. D. (2007) *J. Am. Chem. Soc. 129*, 7740–7741.
19. Thibodeaux, C. J., Mansoorabadi, S. O., Kittleman, W., Chang, W. C., and Liu, H. W. (2008) *Biochemistry 47*, 2547–2558.
20. Walker, J. R., Rothman, S. C., and Poulter, C. D. (2008) *J. Org. Chem. 73*, 726–729.
21. DeLano, W. L. (2002) *The PyMOL Molecular Graphics System*, 0.99rev8, DeLano Scientific, San Carlos, CA.

BI801159X